

Effects of simulated Secondary Organic Aerosol Water on fine PM levels and composition over US

Commented [S1]: Reviewer 1 Comment 4

Stylios Kakavas^{1,2}, Spyros N. Pandis^{1,2} and Athanasios Nenes^{1,3}

¹Institute of Chemical Engineering Sciences, Foundation for Research and Technology Hellas, Patras, Greece

²Department of Chemical Engineering, University of Patras, Patras, Greece

³School of Architecture, Civil and Environmental Engineering, École Polytechnique Fédérale de Lausanne (EPFL), Switzerland

Correspondence to: Spyros N. Pandis (spyros@chemeng.upatras.gr) and Athanasios Nenes (athanasios.nenes@epfl.ch).

Abstract. Water is a key component of atmospheric aerosol, affecting many aerosol processes including gas/particle partitioning of semi-volatile compounds. Water related to secondary organic aerosol (SOAW) is often neglected in atmospheric chemical transport models and is not considered in gas-to-particle partitioning calculations for inorganic species. We use a new inorganic aerosol thermodynamics model, ISORROPIA-lite, which considers the effects of SOAW, to perform chemical transport model simulations for a year over the continental United States to quantify its effects on aerosol mass concentration and composition. SOAW can increase average fine aerosol water levels up to a factor of two when secondary organic aerosol (SOA) is a major PM₁ component. This is often the case in the south-eastern U.S where SOA concentrations are higher. Although the annual average impact of this added water on total dry PM₁ concentrations due to increased partitioning of nitrate and ammonium is small (up to 0.1 µg m⁻³), total dry PM₁ increases of up to 2 µg m⁻³ (with nitrate levels increases up to 200%) can occur when RH levels and PM₁ concentrations are high.

1. Introduction

Fine atmospheric particulate matter with aerodynamic diameter smaller than 2.5 µm (PM_{2.5}) has adverse effects on public health, climate and ecosystem productivity (Pye et al., 2020; Baker et al., 2021; Guo et al., 2021). PM_{2.5} is composed of thousands of organic compounds, black carbon (BC), and inorganic components such

Commented [S2]: Reviewer 1 Comment 5

36 as sulfate (SO_4^{2-}), nitrate (NO_3^-), ammonium (NH_4^+) and chloride (Cl^-) (Seinfeld and
37 Pandis, 2006). ~~Potassium (K^+) levels can also be significant during biomass burning~~
38 ~~events (Zhang et al., 2015; Pye et al., 2020).~~ Ambient aerosol is mostly composed of
39 water which is determined by the chemical equilibrium of water vapor with the
40 aerosol constituents (Liao and Seinfeld, 2005; Carlton and Turpin, 2013; [Bian et al.,](#)
41 [2014](#); Guo et al., 2015; Bougiatioti et al., 2016; Nguyen et al., 2016; Guo et al., 2017;
42 [Deetz et al., 2018](#); [Kuang et al., 2018](#); Song et al., 2018; [Wu et al., 2018](#); Pye et al.,
43 [2020](#); [Gopinath et al., 2022](#)). Aerosol liquid water directly affects the PM sensitivity
44 and dry deposition rates, with direct implications for emissions control policy (Nenes
45 et al., 2020; Nenes et al., 2021; Sun et al., 2021).

Commented [Σ3]: Reviewer 1 Comment 6

Commented [Σ4]: Reviewer 2 Comment 4

Commented [Σ5]: Reviewer 1 Comment 13

46 The hygroscopicity parameter (κ), which expresses the ability of a PM
47 component to absorb water, is an effective approach for the parameterization of the
48 water uptake of atmospheric PM that is a mixture of organic and inorganic species
49 (Petters and Kreidenweis, 2007). Although organic aerosol (OA) is less hygroscopic
50 than inorganic salts, it can still contribute significantly to the total aerosol water (Guo
51 et al., 2015; Bougiatioti et al., 2016; Jathar et al., 2016; [Li et al., 2019](#)) or can even
52 become the dominant contributor at lower ambient relative humidity (Jin et al., 2020).
53 Previous studies have demonstrated that secondary organic aerosol (SOA) is a lot
54 more hygroscopic ($0.1 \leq \kappa \leq 0.3$) than primary organic aerosol (POA) ($\kappa \leq 0.01$) and
55 is mainly responsible for the corresponding OA water (Petters et al., 2006; Koehler et
56 al., 2009; Chang et al., 2010; Jathar et al., 2016; Kuang et al., 2020; Li et al., 2020).

Commented [Σ6]: Reviewer 2 Comment 5

Commented [Σ7]: Reviewer 1 Comment 8

Commented [Σ8]: Reviewer 2 Comment 6

Commented [Σ9]: Reviewer 2 Comment 3

57
58 SOAW can enhance secondary inorganic aerosol concentrations assisting in
59 their partitioning in the particulate phase to satisfy equilibrium. However, such effects
60 are not considered in thermodynamic modules used for the simulation of gas-to-
61 particle partitioning of inorganic species in chemical transport models. Evidence
62 exists however that fine aerosol nitrate and ammonium concentrations can increase in
63 areas with high organic aerosol and RH levels (Kakavas et al., 2022). The importance
64 of these SOAW impacts on secondary aerosol formation s has not been systematically
65 studied and is the focus of this work.

Commented [Σ10]: Reviewer 2 Comment 7

66 We use a new aerosol thermodynamics model, ISORROPIA-lite (Kakavas et
67 al., 2022), to simulate SOAW effects on the partitioning of the inorganic components,
68 for a year over the continental United States. The model performance has been
69 evaluated for fine PM and its components for the examined period by Skyllakou et al.

70 (2021). Its predictions were compared against PM_{2.5} composition measurements from
71 approximately 300 stations of the CSN and IMPROVE networks and PM_{2.5} mass
72 concentrations from 1067 stations. The PMCAMx performance was found to be ~~It is~~
73 ~~considered~~ good for the total PM_{2.5} concentration (fractional bias less than 30% and
74 fractional error less than 50%) and average (fractional bias less than 60% and
75 fractional error less than 75%) for its major~~most of the~~ components. Details about the
76 evaluation can be found in Skyllakou et al. (2021). The aim of our work is to quantify
77 the SOAW contribution to the total fine PM water and to study its effects on inorganic
78 aerosol thermodynamics and total dry fine PM levels and composition.

Commented [Σ11]: Reviewer 1 Comment 2

80 2. Methods

81 2.1 ISORROPIA-lite

82 ISORROPIA-lite is a lean and accelerated version of the widely used ISORROPIA-II
83 (Fountoukis and Nenes, 2007) aerosol thermodynamics model. It assumes that the
84 aerosol exists only in the metastable state at low RH and the activity coefficients of
85 ionic pairs are always obtained from precalculated look-up tables. It estimates aerosol
86 water associated with each one of the aerosol components. Furthermore,
87 ISORROPIA-lite has an important additional feature compared to ISORROPIA-II, as
88 it considers the effects of SOAW on inorganic aerosol thermodynamics. The resulting
89 increase of the total water mass drives more of the water-soluble gaseous species to
90 the particle phase to satisfy equilibrium. SOAW, W_{SOA} , in ISORROPIA-lite is
91 calculated using the well-established κ -Kohler theory of Petters and Kreidenweis
92 (2007):

$$93 \quad W_{SOA} = \frac{\rho_w}{\rho_{SOA}} \frac{C_{SOA} \kappa}{\left(\frac{1}{RH} - 1\right)} \quad (1)$$

94 where ρ_w is the density of water, ρ_{SOA} the SOA density, C_{SOA} the SOA concentration, κ
95 the SOA hygroscopicity parameter and RH the relative humidity in the 0–1 scale.
96 More details about the ISORROPIA-lite can be found in Kakavas et al. (2022).

98 2.2 PMCAMx description and application

99 PMCAMx (Karydis et al., 2010; Tsimpidi et al., 2010) is a three dimensional
100 chemical transport model based on CAMx (Environ, 2006), which simulates
101 horizontal and vertical advection and dispersion, dry and wet deposition, as well as

102 aqueous, gas, and aerosol chemistry. The mechanism used in this work for gas-phase
103 chemistry simulations is the Carbon Bond 05 (CB5) (Yarwood et al., 2005) and
104 includes 190 reactions of 79 gas species. To describe the aerosol size and composition
105 distribution 10-size sections (from 40 nm to 40 μm) are used assuming that all
106 particles in each size bin have the same composition. [Therefore, PMCAMx predicts](#)
107 [the PM_x concentrations where x can be among other choices 1, 2.5 and 10 \$\mu\text{m}\$.](#)
108 Equilibrium is always assumed between the bulk aerosol and gas phases. The
109 partitioning of semi-volatile inorganic species between the gas and particulate phases
110 is simulated by ISORROPIA-lite. Weighting factors based on each size bin's effective
111 surface area are used to distribute to the various size bins the mass transferred
112 between the two phases in each time step (Pandis et al., 1993). For the simulation of
113 organic aerosols, the volatility basis set approach (Donahue et al., 2006) is used. POA
114 is simulated using eight volatility bins (from 10^{-1} to $10^6 \mu\text{g m}^{-3}$) at 298 K, while for
115 SOA four volatility bins (1, 10, 10^2 , $10^3 \mu\text{g m}^{-3}$) at 298 K are used (Murphy and
116 Pandis, 2009). For the major point sources, the NO_x plumes are simulated using the
117 Plume-in-Grid (PiG) approach (Karamchandani et al., 2011; Zakoura and
118 Pandis, 2019).

Commented [Σ12]: Reviewer 1 Comment 5

119 We applied PMCAMx over the continental United States during 2010. The
120 modeling domain includes northern Mexico and southern Canada and covers a $4752 \times$
121 2952 km^2 region (Figure S1). The model grid consists of 10,824 cells with horizontal
122 dimensions of $36 \times 36 \text{ km}$. The meteorological inputs were provided by the Weather
123 Research Forecasting model (WRF v3.6.1) using a horizontal resolution of $12 \times$
124 12 km . [While it is difficult to measure accurately RH values above 95%, model](#)
125 [predictions are more reliable. Therefore, ~~Therefore, RH levels do not suffer from the~~](#)
126 [corresponding experimental challenges and there was no need for screening of the few](#)
127 [RH values above 95%.](#) The gaseous and primary particle emissions were developed
128 by Xing et al. (2013). More details about the meteorological inputs and the emissions
129 can be found in Skyllakou et al. (2021).

Commented [Σ13]: Reviewer 1 Comment 11

130 To quantify the SOAW effects on inorganic aerosol thermodynamics three
131 simulations were performed. The first was a simulation neglecting SOAW and
132 including only inorganic aerosol water. ~~Two~~ two additional simulations were
133 performed: one where κ of SOA was assumed to be equal to 0.1 and one with $\kappa=0.2$ to
134 examine how SOA hygroscopicity affects total fine aerosol water content and PM
135 levels and composition. [Previous studies have estimated secondary organic aerosol](#)

136 density values of 1–1.4 g cm⁻³ (Turpin and Lim, 2001; Konstenidou et al., 2007). A
137 SOA density of 1 g cm⁻³ was assumed in the simulations. ~~H~~because higher densities
138 suggest that SOA particles may be in a ~~in~~-solid or waxy state (Konstenidou et al.,
139 2007). ~~The~~ SOA exists mostly in submicrometer particles so our subsequent study
140 focuses on PM₁.

Commented [Σ14]: Reviewer 1 Comment 2

Commented [Σ15]: Reviewer 1 Comment 9

141

142 3. Results

143 3.1 Effects of SOAW on PM₁ water levels

144 The annual average PM₁ water ground-level concentrations neglecting SOAW are
145 shown in Figure 1. Higher PM₁ water concentrations from 8 to 18 μg m⁻³ are
146 predicted in the north-eastern part of the US due to the higher inorganic PM₁
147 concentrations (Figure S2) and RH levels in that area. When SOAW is present in the
148 simulations, total PM₁ water levels increase everywhere with higher fractional
149 increases in the south-eastern US (up to 50% when κ=0.1 and up to 100% when κ=0.2
150 in Alabama and north-western Mexico) due to higher SOA levels (Figure S23). In the
151 north-eastern US, lower fractional increases are predicted (10–15% when κ=0.1 and
152 20–30% when κ=0.2). In general, assuming a κ of SOA equal to 0.2 instead of 0.1
153 increases the corresponding amount of SOAW by about a factor of two. Figure 1
154 shows the distributions of fractional increase change in the annual PM₁ water levels at
155 ground level from SOAW. Total PM₁ water average concentrations increase from 20
156 to 30% in about 60% of the modeling domain when κ=0.1. For κ=0.2, the
157 corresponding increase is from 40 to 60%.

158 Predicted SOA levels are higher during summertime (Figure S23) since the
159 emissions and oxidation rates of volatile organic compounds (VOCs) are higher
160 (Zhang et al., 2013; Freney et al., 2014; Skyllakou et al., 2014; Fountoukis et al.,
161 2016). However, even during wintertime fresh biomass burning emissions exposed to
162 NO₂ and O₃ can form significant amounts of SOA in periods with low OH levels
163 (Kodros et al., 2020). Higher total PM₁ water concentrations are predicted during
164 winter (Figure 3S4) since the RH levels and inorganic fine aerosol concentrations are
165 higher; especially nitrate and chloride which increasingly partition to the aerosol
166 phase as temperature decreases (Guo et al., 2017). ~~Predicted~~ ~~However, average PM₁~~
167 ~~chloride concentrations are low (less than 0.1 μg m⁻³) in all areas, with higher~~
168 ~~concentrations in parts of Kansas because of biomass burning in the simulated period~~
169 ~~episodes~~. Higher fractional increases in fine aerosol water levels (up to 5 times) due to

Commented [Σ16]: Reviewer 1 Comment 7

170 SOAW are predicted during summer in the south-eastern part of US where SOA
171 concentrations are higher. This corresponds to increases to average fine aerosol water
172 concentrations up to $8 \mu\text{g m}^{-3}$.

173 Ammonium nitrate and ammonium sulfate are the inorganic salts that
174 contribute the most to the total PM_{10} water levels (Figure S35). SOAW also
175 contributes significantly to the total PM_{10} water levels especially in the south-eastern
176 US (about 30 and 50% of total PM_{10} water when $\kappa=0.1$ and $\kappa=0.2$ respectively), when
177 the mass fraction of SOA in dry PM_{10} exceeds 30%.

178

179 3.2 Effects of SOAW on total dry PM_{10} levels

180 Higher dry PM_{10} concentrations are predicted for the eastern part of the US (up to 15
181 $\mu\text{g m}^{-3}$) in the base case (Figure 42). These dry PM_{10} levels increase slightly up to
182 0.6% and 1.2% due to SOAW when $\kappa=0.1$ and $\kappa=0.2$ for SOA is assumed. The
183 highest annual average fractional increase in total dry PM_{10} levels is predicted in
184 California (1% when $\kappa=0.1$ and 2% when $\kappa=0.2$). The probability density (Figure 42)
185 indicates that in about 60% of the modeling domain total dry fine aerosol
186 concentrations increase up to 0.3% when $\kappa=0.1$. For $\kappa=0.2$, the corresponding increase
187 is from 0.4 to 2%. The areas of the highest PM_{10} increase correspond to regions where
188 aerosol pH tends to be relatively high (Pye et al., 2020). In these areas, nitric acid and
189 ammonia can condense and increase aerosol mass because of the increase in water
190 from the SOA. Because of this partitioning change, the predicted gas-phase
191 concentrations of semi-volatile inorganic components decreased on average when
192 SOAW was considered (Figure S46). SOAW had a negligible absolute impact on the
193 small fine chloride concentrations in this period (Figure S2). However, in periods
194 during which chloride salts and SOA contribute significantly to the total dry (e.g.
195 during intense biomass burning periods), fine chloride concentrations could also
196 change (Metzger et al., 2006; Fountoukis et al., 2009; Gunthe et al., 2021).

197 [Syllakou et al. \(2021\)](#) found that PMCAMx had a small fractional bias (5%)
198 and a fractional error (25%) for the annual average $\text{PM}_{2.5}$ concentrations of 1067
199 measurements stations in the U.S. ~~The performance of PMCAMx regarding for annual~~
200 ~~average OA was similar (-is considered good in these simulations with a fractional~~
201 ~~bias of 5% and a fractional error of 26%) in the 306 stations in the US. For daily~~
202 ~~average concentrations the performance is also quite encouraging with a fractional~~
203 ~~bias of 15% and a fractional error of 56%. Given that the addition of SOAW to the~~

Commented [S17]: Reviewer 1 Comment 12

204 model had a small effect on the dry fine PM mass (of the order of 1%) there was no
205 of the extension of the model on the total fine PM mass is small (of the order of 1%);
206 this does not result in any noticeable change in the its already very good performance
207 of the model for dry fine PM. Therefore, the major change in the model predictions is
208 on the aerosol water concentrations.

Commented [Σ18]: Reviewer 2 Comment 2

Commented [Σ19]: Reviewer 1 Comment 12

209
210

211 3.3 Effects of SOAW on PM₁ components

212 The annual average results indicate that SOAW mainly affects fine aerosol water
213 levels. To better analyze the effects of SOAW we focus on the temporal evolution of
214 the predicted levels of PM₁ components in four sites (Figure S1) with different
215 characteristics (Table S1). We have chosen one city from the West, one from the
216 South, one from Southeast and one from the Northeast. They are all in different
217 environments with different major sources and climatological conditions. The
218 presence of SOAW increased PM₁ water concentrations in all sites from 1% to almost
219 an order of magnitude (Figure 53). However, these fractional increases most of the
220 time correspond to PM₁ water concentration increases of a few $\mu\text{g m}^{-3}$ (Figure 6S7)
221 because they occur under low RH levels. During higher RH periods (80 to 100%), the
222 PM₁ water levels are predicted to increase up to $100 \mu\text{g m}^{-3}$ (e.g. in Toronto).

Commented [Σ20]: Reviewer 1 Comment 10

223 Total dry PM₁ concentrations during most of the simulated period increase on
224 average less than 1% in all sites (Figure 53) due to SOAW. There are periods,
225 however, with higher fractional increases (up to 10%) and even small decreases (up to
226 5%) in total dry fine aerosol levels in the examined sites. The decreases can be
227 explained because SOAW increases the size of particles and therefore their dry
228 deposition rate (Nenes et al., 2020). Depending on SOA hygroscopicity, increases up
229 to $1.5 \mu\text{g m}^{-3}$ for nitrate and $0.5 \mu\text{g m}^{-3}$ for ammonium are predicted (Figure 6S7).
230 Fine nitrate increases of 10% were more frequent in the examined sites; however
231 higher increases up to 200% are predicted during the simulated period (Figure 74). As
232 expected, higher increases can occur more often with higher assumed SOA
233 hygroscopicity.

234

235 4. Discussion and Conclusions

236 Aerosol liquid water has a profound impact on aerosol processes, chemical
237 composition and their impacts. By including the effects of organic water on

238 inorganics thermodynamic equilibrium we show that SOAW can substantially
239 increase aerosol water levels, on an average up to 60% over the majority of the
240 domain. As a consequence, total dry PM₁ levels can also increase but the changes are
241 small (up to 2% on an annual average basis). Locally these effects can be much more
242 significant during periods of high RH and SOA levels (fine nitrate fractional increases
243 can be as high as 200%).

244 The effects vary with season. During summer, the RH is lower and SOA levels
245 are higher leading to higher fractional increases in aerosol water (Figure 3S4) but
246 lower absolute mass changes. During summer the fractional increases in total dry fine
247 aerosol concentrations are lower than in wintertime (Figure S58). Responsible for the
248 total dry fine aerosol concentration increases are nitrate and ammonium (Figure S2).
249 These compounds partition together (as deliquesced ammonium nitrate) to the
250 particulate phase to satisfy equilibrium due to the additional water mass of SOA.

251 The increases in total dry PM₁ and fine aerosol water levels depend on SOA
252 concentrations, hygroscopicity value, RH levels and the particle phase fractions of
253 inorganic species. The SOAW effect on aerosol water is approximately proportional
254 to the assumed hygroscopicity parameter κ . Given that our work investigates the
255 potential significance of this effect we have chosen to provide the results of two
256 simulations one with relatively low and one with relatively high hygroscopicity of
257 SOA. A more detailed treatment of the hygroscopicity parameter (e.g., assigning a
258 different value to each OA component) will be a topic of future work.

Commented [Σ21]: Reviewer 1 Comment 9

259 ~~Aerosol liquid water directly affects the PM sensitivity and dry deposition~~
260 ~~rates, with direct implications for emissions control policy (Nenes et al., 2020; Nenes~~
261 ~~et al., 2021; Sun et al., 2021).~~ Given this, and the important role of The present work,

Commented [Σ22]: Reviewer 1 Comment 13

262 thoroughly analyzes organic water uptake impacts over one simulated year (not just
263 one month as done in Kakavas et al., 2022) and in quite a different geographical area
264 (US here versus Europe in Kakavas et al., 2022). There are significant differences, but
265 also similarities in the predicted changes and effects of SOA water. Both studies
266 indicate that SOAW can contribute highly significantly to the total PM₁ water and
267 increase particulate nitrate concentrations especially in areas with high total nitrate
268 concentrations. Given this, and the important role of SOAW for climate forcing,

Commented [Σ23]: Reviewer 2 Comment 1

269 visibility and chemistry, its inclusion in future studies is highly recommended.
270 ISORROPIA-lite provides a simple and computationally effective approach for the
271 simulation of SOAW.

Commented [Σ24]: Reviewer 1 Comment 14

272

273 **Code and Data Availability.** The model code and data used in this study are available
274 from the authors upon request (spyros@chemeng.upatras.gr and
275 athanasios.nenes@epfl.ch).

276

277 **Author Contributions.** SK incorporated ISORROPIA-lite in PMCAMx, carried out the
278 simulations, analyzed the results and wrote the manuscript. SN and AN conceived and
279 led the study and helped in the writing of the manuscript.

280

281 **Competing Interests.** The authors declare no competing financial interest.

282

283 **Acknowledgements.** This work was supported by the project FORCeS funded from
284 the European Union's Horizon 2020 research and innovation programme under grant
285 agreement No 821205, and project PyroTRACH (ERC-2016-COG) funded from
286 H2020-EU.1.1. - Excellent Science - European Research Council (ERC), project ID
287 726165.

288

289 **References**

290 Baker, A., Kanakidou, M., Nenes, A., Myriokefalitakis, S., Croot, P.L., Duce, A. D.,
291 Gao, Y., Guieu, C., Ito, A., Jickells, T. D., Mahowald, N. M., Middag, R.,
292 Perron, M. M. G., Sarin, M. M., Shelley, R., and Turner, D. R.: Changing
293 atmospheric acidity as a modulator of nutrient deposition and ocean
294 biogeochemistry, *Sci. Adv.*, 7, doi: 10.1126/sciadv.abd8800, 2021.

295 [Bian, Y. X., Zhao, C. S., Ma, N., Chen, J., and Xu, W. Y.: A study of aerosol liquid
296 water content based on hygroscopicity measurements at high relative humidity
297 in the North China Plain, *Atmos. Chem. Phys.*, 14, 6417–6426, 2014.](#)

298 Bougiatioti, A., Nikolaou, P., Stavroulas, I., Kouvarakis, G., Weber, R., Nenes, A.,
299 Kanakidou, M., and Mihalopoulos, N.: Particle water and pH in the eastern
300 Mediterranean: source variability and implications for nutrient availability,
301 *Atmos. Chem. Phys.*, 16, 4579–4591, 2016.

302 Carlton, A. G. and Turpin, B. J.: Particle partitioning potential of organic compounds
303 is highest in the Eastern US and driven by anthropogenic water, *Atmos. Chem.
304 Phys.*, 13, 10203–10214, 2013.

305 [Chang, R. Y.-W., Slowik, J. G., Shantz, N. C., Vlasenko, A., Liggio, J., Sjostedt, S. J.,](#)
306 [Leaitch, W. R., and Abbatt, J. P. D.: The hygroscopicity parameter \(\$\kappa\$ \) of](#)
307 [ambient organic aerosol at a field site subject to biogenic and anthropogenic](#)
308 [influences: relationship to degree of aerosol oxidation, *Atmos. Chem. Phys.*,](#)
309 [10, 5047–5064, 2010.](#)

310 [Deetz, K., Vogel, H., Haslett, S., Knippertz, P., Coe, H., and Vogel, B.: Aerosol liquid](#)
311 [water content in the moist southern West African monsoon layer and its](#)
312 [radiative impact, *Atmos. Chem. Phys.*, 18, 14271–14295, 2018.](#)

313 Donahue, N. M., Robinson, A. L., Stanier, C. O., and Pandis, S. N.: Coupled
314 partitioning, dilution, and chemical aging of semivolatile organics, *Environ.*
315 *Sci. Technol.*, 40, 2635–2643, 2006.

316 Environ: Comprehensive Air Quality Model with Extensions Version 4.40. Users
317 Guide. ENVIRON Int. Corp., Novato, CA, <http://www.camx.com>, 2006.

318 Fountoukis, C. and Nenes, A.: ISORROPIA II: a computationally efficient
319 thermodynamic equilibrium model for K^+ - Ca^{2+} - Mg^{2+} - NH_4^+ - Na^+ - SO_4^{2-} - NO_3^- -
320 Cl^- - H_2O aerosols, *Atmos. Chem. Phys.*, 7, 4639–4659, 2007.

321 Fountoukis, C., Nenes, A., Sullivan, A., Weber, R., Van Reken, T., Fischer, M.,
322 Matías, E., Moya, M., Farmer, D., and Cohen, R. C.: Thermodynamic
323 characterization of Mexico City aerosol during MILAGRO 2006, *Atmos.*
324 *Chem. Phys.*, 9, 2141–2156, 2009.

325 Fountoukis, C., Megaritis, A. G., Skyllakou, K., Charalampidis, P. E.,
326 Denier van der Gon, H. A. C., Crippa, M., Prévôt, A. S. H., Fachinger, F.,
327 Wiedensohler, A., Pilinis, C., and Pandis, S. N.: Simulating the formation of
328 carbonaceous aerosol in a European Megacity (Paris) during the MEGAPOLI
329 summer and winter campaigns, *Atmos. Chem. Phys.*, 16, 3727–3741, 2016.

330 Freney, E. J., Sellegri, K., Canonaco, F., Colomb, A., Borbon, A., Michoud, V.,
331 Doussin, J.-F., Crumeyrolle, S., Amarouche, N., Pichon, J.-M., Bourianne, T.,
332 Gomes, L., Prevot, A. S. H., Beekmann, M., and Schwarzenböeck, A.:
333 Characterizing the impact of urban emissions on regional aerosol particles:
334 airborne measurements during the MEGAPOLI experiment, *Atmos. Chem.*
335 *Phys.*, 14, 1397–1412, 2014.

336 [Gopinath, A. K., Raj, S. S., Kommula, S. M., Jose, C., Panda, U., Bishambu, Y.,](#)
337 [Ojha, N., Ravikrishna, R., Liu, P., and Gunthe, S. S.: Complex i](#)[nterplay](#)

338 [bBetween oOrganic and sSecondary iInorganic aAerosols wWith aAmbient](#)
339 [rRelative hHumidity iImplicates the aAerosol LLiquid wWater cContent oOver](#)
340 [India dDuring wWintertime. J.ournal of Geophys.ical Res.earch:](#)
341 [Atmospheres. 127,\(13\), e2021JD036430, 2022.](#)

342 Gunthe, S. S., Liu, P., Panda, U., Raj, S. S., Sharma, A., Derbyshire, E., Reyes-
343 Villegas E., Allan, J., Chen, Y., Wang, X., Song, S., Pöhlker, M. L., Shi, L.,
344 Wang, Y., Kommula, S. M., Liu, T., Ravikrishna, R., McFiggans, G., Mickey,
345 L. J., Martin, S. T., Pöschl, U., Andreae, M. O., and Coe, H.: Enhanced
346 aerosol particle growth sustained by high continental chlorine emission in
347 India., *Nat. Geosci.*, 14, 77–84, 2021.

348 Guo, H., Xu, L., Bougiatioti, A., Cerully, K. M., Capps, S. L., Hite Jr., J. R., Carlton,
349 A. G., Lee, S.-H., Bergin, M. H., Ng, N. L., Nenes, A., and Weber, R. J.: Fine-
350 particle water and pH in the southeastern United States, *Atmos. Chem. Phys.*
351 15, 5211–5228, 2015.

352 Guo, H., Liu, J., Froyd, K. D., Roberts, J. M., Veres, P. R., Hayes, P. L., Jimenez, J.
353 L., Nenes, A., and Weber, R. J.: Fine particle pH and gas–particle phase
354 partitioning of inorganic species in Pasadena, California, during the 2010
355 CalNex campaign, *Atmos. Chem. Phys.*, 17, 5703–5719, 2017.

356 Guo, H., Li, X., Li, W., Wu, J., Wang, S., and Wei, J.: Climatic modification effects
357 on the association between PM₁ and lung cancer incidence in China, *BMC*
358 *public health*, 21, 880, 2021.

359 Jathar, S.H., Mahmud, A., Barsanti, K.C., Asher, W. E., Pankow, J. F., and Kleeman
360 M. J.: Water uptake by organic aerosol and its influence on gas/particle
361 partitioning of secondary organic aerosol in the United States, *Atmos.*
362 *Environ.*, 129, 142–154, 2016.

363 Jin, X., Wang, Y., Li, Z., Zhang, F., Xu, W., Sun, Y., Fan, X., Chen, G., Wu, H., Ren,
364 J., Wang, Q., and Cribb, M.: Significant contribution of organics to aerosol
365 liquid water content in winter in Beijing, China, *Atmos. Chem. Phys.*, 20,
366 901–914, 2020.

367 Kakavas, S., Pandis, S. N., and Nenes, A.: ISORROPIA-lite: A comprehensive
368 atmospheric aerosol thermodynamics module for Earth System Models, *Tellus*
369 *B*, 74, 1–23, 2022.

370 Karamchandani, P., Vijayaraghavan, K., and Yarwood, G.: Sub-grid scale plume
371 modeling, *Atmosphere*, 2, 389–406, 2011.

372 Karydis, V. A., Tsimpidi, A. P., Fountoukis, C., Nenes, A., Zavala, M., Lei, W.,
373 Molina, L. T., and Pandis, S. N.: Simulating the fine and coarse inorganic
374 particulate matter concentrations in a polluted megacity, *Atmos. Environ.*, 44,
375 608–620, 2010.

376 Kodros, J. K., Papanastasiou, D. K., Paglione, M., Masiol, M., Squizzato, S., Florou,
377 K., Skyllakou, K., Kaltsonoudis, C., Nenes, A., and Pandis, S. N.: Rapid Dark
378 Aging of Biomass Burning as an Overlooked Source of Oxidized Organic
379 Aerosol, *Proc. Natl. Acad. Sci. U.S.A.*, 117, 33028–33033, 2020.

380 Koehler, K. A., Kreidenweis, S. M., DeMott, P. J., Petters, M. D., Prenni, A. J., and
381 Carrico, C. M.: Hygroscopicity and cloud droplet activation of mineral dust
382 aerosol, *Geoph. Res. Lett.*, 36, (8), 2009.

383 [Kostenidou, E., Pathak, R. K., and Pandis, S. N.: An algorithm for the calculation of
384 secondary organic aerosol density combining AMS and SMPS data, *Aerosol
385 Sci. Technol.*, 41, \(11\), 1002–1010, 2007.](#)

386 [Kuang, Y., Zhao, C. S., Zhao, G., Tao, J. C., Xu, W., Ma, N., and Bian, Y. X.: A
387 novel method for calculating ambient aerosol liquid water content based on
388 measurements of a humidified nephelometer system, *Atmospheric
389 Measurement Techniques*, 11, 2967–2982, 2018.](#)

390 [Kuang, Y., Xu, W., Tao, J., Ma, N., Zhao, C., and Shao, M.: A review on laboratory
391 studies and field measurements of atmospheric organic aerosol hygroscopicity
392 and its parameterization based on oxidation levels, *Current Pollution Reports*,
393 10.1007/s40726-020-00164-2, 2020.](#)

394 [Li, X., Song, S., Zhou, W., Hao, J., Worsnop, D. R., and Jiang, J.: Interactions
395 between aerosol organic components and liquid water content during haze
396 episodes in Beijing, *Atmos. Chem. Phys.*, 19, 12163–12174, 2019.](#)

397 [Li, J., Zhang, H., Ying, Q., Wu, Z., Zhang, Y., Wang, X., Li, X., Sun, Y., Hu, M.,
398 Zhang, Y., and Hu, J.: Impacts of water partitioning and polarity of organic
399 compounds on secondary organic aerosol over eastern China, *Atmos. Chem.
400 Phys.*, 20, 7291–7306, 2020.](#)

401 Liao, H. and Seinfeld, J. H.: Global impacts of gas-phase chemistry aerosol
402 interactions on direct radiative forcing by anthropogenic aerosols and ozone, *J.
403 Geophys. Res.*, 110, D18208, 2005.

404 Metzger, S., Mihalopoulos, N., and Lelieveld, J.: Importance of mineral cations and
405 organics in gas-aerosol partitioning of reactive nitrogen compounds: case
406 study based on MINOS results., *Atmos. Chem. Phys.*, 6, 2549–2567, 2006.

407 Murphy, B. N. and Pandis, S. N.: Exploring summertime organic aerosol formation in
408 the Eastern United States using a regional-scale budget approach and ambient
409 measurements, *J. Geophys. Res.*, 115, (D24216), 2010.

410 Nenes, A., Pandis, S. N., Weber, R. J., and Russell, A.: Aerosol pH and liquid water
411 content determine when particulate matter is sensitive to ammonia and nitrate
412 availability, *Atmos. Chem. Phys.*, 20, 3249–3258, 2020.

413 Nenes, A., Pandis, S. N., Kanakidou, M., Russell, A. G., Song, S., Vasilakos, P., and
414 Weber, R. J.: Aerosol acidity and liquid water content regulate the dry
415 deposition of inorganic reactive nitrogen, *Atmos. Chem. Phys.*, 21, 6023–
416 6033, 2021.

417 Nguyen, T. K. V., Zhang, Q., Jimenez, J. L., Pike, M., and Carlton, A. G.: Liquid
418 water: ubiquitous contributor to aerosol mass. *Environ. Sci. Tech. Lett.*, 3,
419 257–263, 2016.

420 Pandis, S. N., Wexler, A. S., and Seinfeld, J. H.: Secondary organic aerosol formation
421 and transport – II. Predicting the ambient secondary organic aerosol size
422 distribution, *Atmos. Environ.*, 27, 2403–2416, 1993.

423 [Petters, M. D., Prenni, A. J., Kreidenweis, S. M., DeMott, P. J., Matsunaga, A., Lim,
424 Y. B., and Ziemann, P. J.: Chemical aging and the hydrophobic-to-hydrophilic
425 conversion of carbonaceous aerosol, *Geophys. Res. Lett.*, 33, L24806, 2006.](#)

426 Petters, M. D. and Kreidenweis, S. M.: A single parameter representation of
427 hygroscopic growth and cloud condensation nucleus activity, *Atmos. Chem.
428 Phys.*, 7, 1961–1971, 2007.

429 Pye, H. O. T., Nenes, A., Alexander, B., Ault, A. P., Barth, M. C., Clegg, S. L.,
430 Collett Jr, J. L., Fahey, K. M., Hennigan, C. J., Herrmann, H., Kanakidou, M.,
431 Kelly, J. T., Ku, I.-T., McNeill, V. F., Riemer, N., Schaefer, T., Shi, G.,
432 Tilgner, A., Walker, J. T., Wang, T., Weber, R., Xing, J., Zaveri, R. A., and
433 Zuend, A.: The acidity of atmospheric particles and clouds, *Atmos. Chem.
434 Phys.*, 20, 4809–4888, 2020.

435 Seinfeld, J. H. and Pandis, S. N.: *Atmospheric chemistry and physics: From air
436 pollution to climate change*, Wiley: New York, 2006.

437 Skyllakou, K., Murphy, B. N., Megaritis, A. G., Fountoukis, C., and Pandis, S. N.:
438 Contributions of local and regional sources to fine PM in the megacity of
439 Paris, *Atmos. Chem. Phys.*, 14, 2343–2352, 2014.

440 Skyllakou, K., Rivera, P. G., Dinkelacker, B., Karnezi, E., Kioutsioukis, I.,
441 Hernandez, C., Adams, P. J., and Pandis, S. N.: Changes in
442 PM_{2.5} concentrations and their sources in the US from 1990 to 2010, *Atmos.*
443 *Chem. Phys.*, 21, 17115–17132, 2021.

444 Song, S., Gao, M., Xu, W., Shao, J., Shi, G., Wang, S., Wang, Y., Sun, Y., and
445 McElroy, M. B.: Fine-particle pH for Beijing winter haze as inferred from
446 different thermodynamic equilibrium models, *Atmos. Chem. Phys.*, 18, 7423–
447 7438, 2018.

448 Sun, X., Ivey, C. E., Baker, K. R., Nenes, A., Lareau, N. P., and Holmes, H. A.:
449 Confronting Uncertainties of Simulated Air Pollution Concentrations during
450 Persistent Cold Air Pool Events in the Salt Lake Valley, Utah., *Environ. Sci.*
451 *Technol.*, 55, 15072–15081, 2021.

452 Tsimpidi, A. P., Karydis, V. A., Zavala, M., Lei, W., Molina, L., Ulbrich, I. M.,
453 Jimenez, J. L., and Pandis, S. N.: Evaluation of the volatility basis-set
454 approach for the simulation of organic aerosol formation in the Mexico City
455 metropolitan area, *Atmos. Chem. Phys.*, 10, 525–546, 2010.

456 [Turpin, B. J. and Lim, H. J.: Species Contributions to PM_{2.5} mMass Concentrations:
457 rRevisiting cCommon aAssumptions for eEstimating oOrganic
458 mMass. *Aerosol Sci. Technol.*, 35, \(4\), 602–610, 2001.](#)

459 [Wu, Z., Wang, Y., Tan, T., Zhu, Y., Li, M., Shang, D., Wang, H., Lu, K., Guo, S.,
460 Zeng, L., and Zhang, Y.: Aerosol liquid water driven by anthropogenic
461 inorganic salts: Implying its key role in haze formation over the North China
462 Plain. *Environmental Science & Technology Letters*,
463 \[10.1021/acs.estlett.8b00021\]\(https://doi.org/10.1021/acs.estlett.8b00021\), 2018.](#)

464 Xing, J., Pleim, J., Mathur, R., Pouliot, G., Hogrefe, C., Gan, C.-M., and Wei, C.:
465 Historical gaseous and primary aerosol emissions in the United States from
466 1990 to 2010, *Atmos. Chem. Phys.*, 13, 7531–7549, 2013.

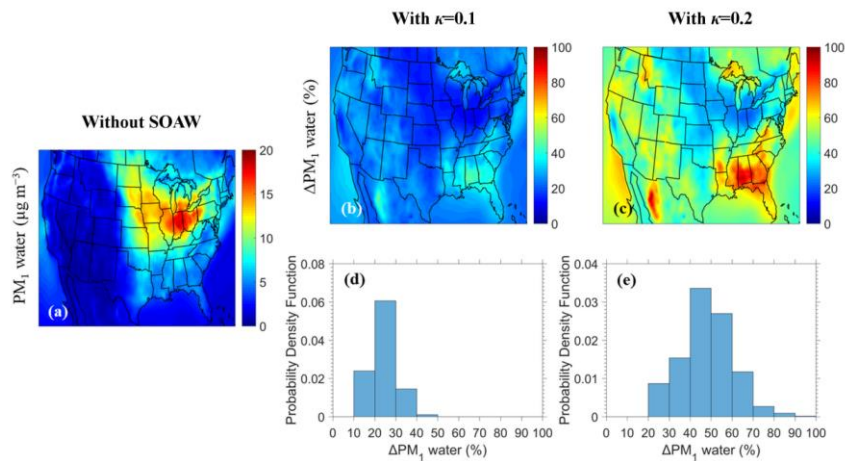
467 Yarwood, G., Rao, S., Yocke, M., and Whitten, G. Z.: Updates to the Carbon Bond
468 Chemical Mechanism: CB05, Research Triangle Park, [https://camx-
469 wp.azurewebsites.net/Files/CB05_Final_Report_120805.pdf](https://camx-wp.azurewebsites.net/Files/CB05_Final_Report_120805.pdf), 2005.

470 Zakoura, M. and Pandis, S. N.: Improving fine aerosol nitrate predictions using a
471 Plume-in-Grid modeling approach, *Atmos. Environ.*, 215, 116887, 2019.

472 Zhang, Q. J., Beekmann, M., Drewnick, F., Freutel, F., Schneider, J., Crippa, M.,
473 Prevot, A. S. H., Baltensperger, U., Poulain, L., Wiedensohler, A., Sciare, J.,
474 Gros, V., Borbon, A., Colomb, A., Michoud, V., Doussin, J.-F., Denier van
475 der Gon, H. A. C., Haeffelin, M., Dupont, J.-C., Siour, G., Petetin, H.,
476 Bessagnet, B., Pandis, S. N., Hodzic, A., Sanchez, O., Honoré, C., and
477 Perrussel, O.: Formation of organic aerosol in the Paris region during the
478 MEGAPOLI summer campaign: evaluation of the volatility basis-set approach
479 within the CHIMERE model, *Atmos. Chem. Phys.*, 13, 5767–5790, 2013.

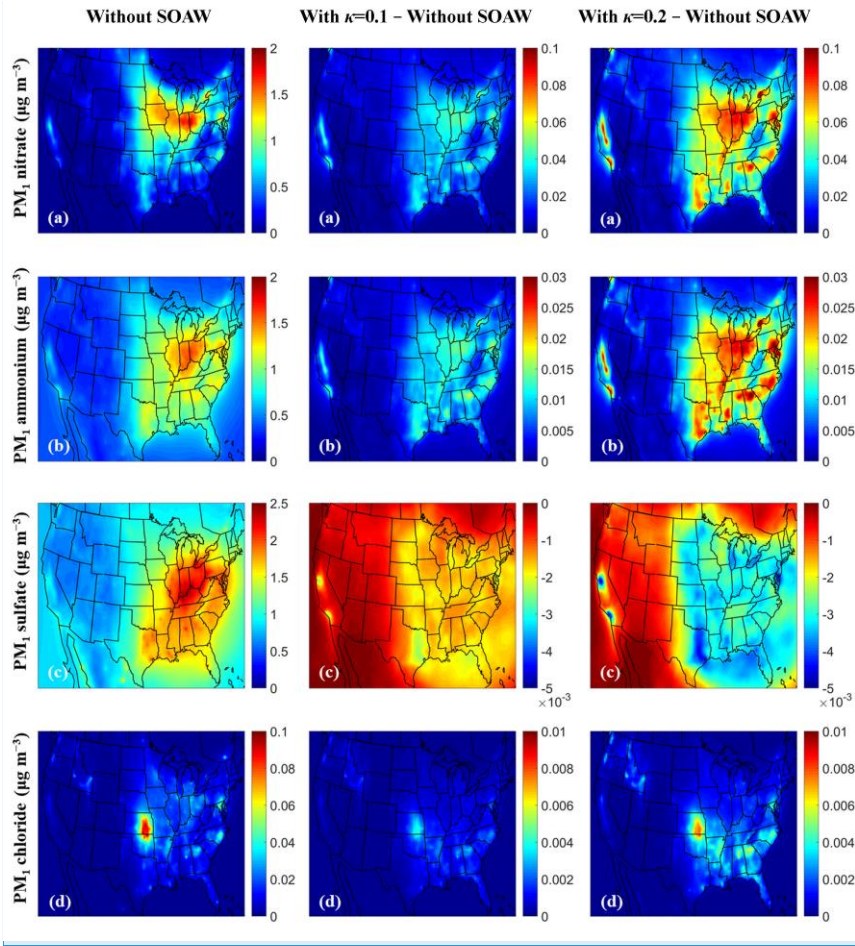
480 ~~Zhang, Z., Gao, J., Engling, G., Tao, J., Chai, F., Zhang, L., Zhang, R., Sang, X.,~~
481 ~~Chan, C., Lin, Z., and Cao, J.: Characteristics and applications of size-~~
482 ~~segregated biomass burning tracers in China's Pearl River Delta region,~~
483 ~~*Atmos. Environ.*, 102, 290–301, 2015.~~

484
485
486
487
488
489
490
491
492
493
494
495
496
497
498
499
500
501
502



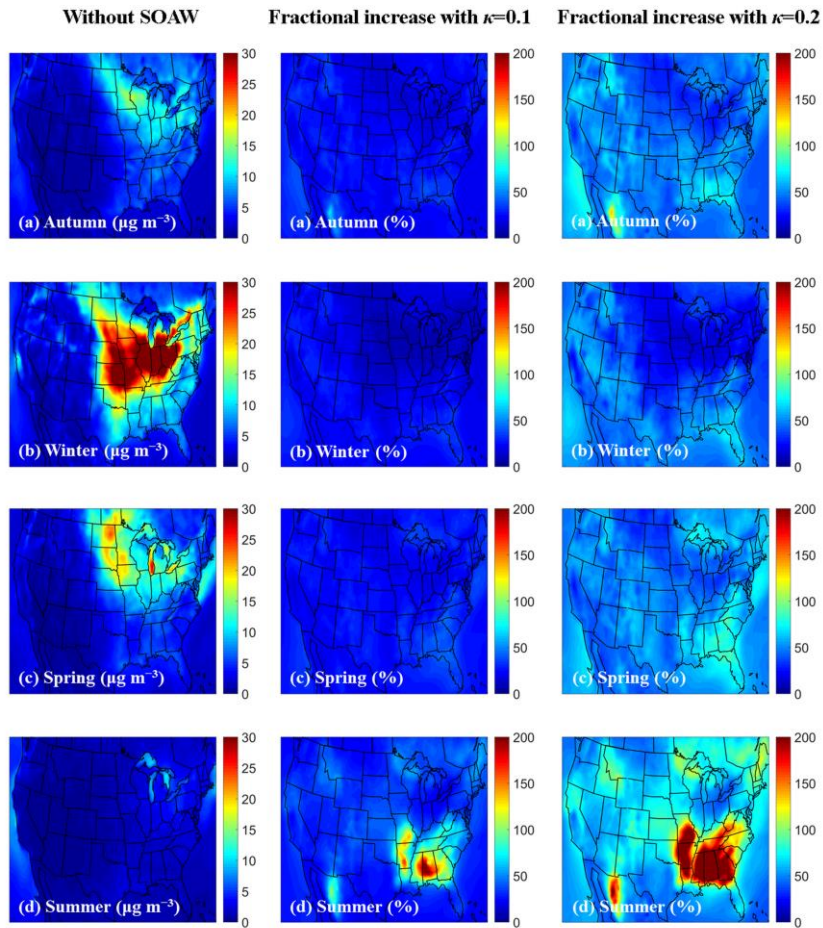
503
 504
 505
 506
 507
 508
 509
 510
 511
 512
 513
 514
 515
 516
 517
 518
 519
 520
 521
 522
 523
 524
 525
 526
 527
 528

Figure 1. Maps of: (a) annual average PM₁ water ground-level concentrations neglecting SOAW, (b) annual average fractional increase of PM₁ water when SOAW is present in the simulations with $\kappa=0.1$ and, (c) with $\kappa=0.2$ during 2010. The probability density as a function of fractional increase in the annual PM₁ water concentrations due to SOAW when: (d) $\kappa=0.1$ and (e) $\kappa=0.2$ is shown.



529
530
531
532
533
534
535
536
537
538
539
540
541

Figure 2. Annual average ground-level concentrations (in $\mu\text{g m}^{-3}$) of PM_{10} : (a) nitrate, (b) ammonium, (c) sulfate, and (d) chloride neglecting SOAW and the annual concentration changes when SOAW is present in the simulations with $\kappa=0.1$ and $\kappa=0.2$. A positive change corresponds to an increase. A negative change corresponds to a decrease.



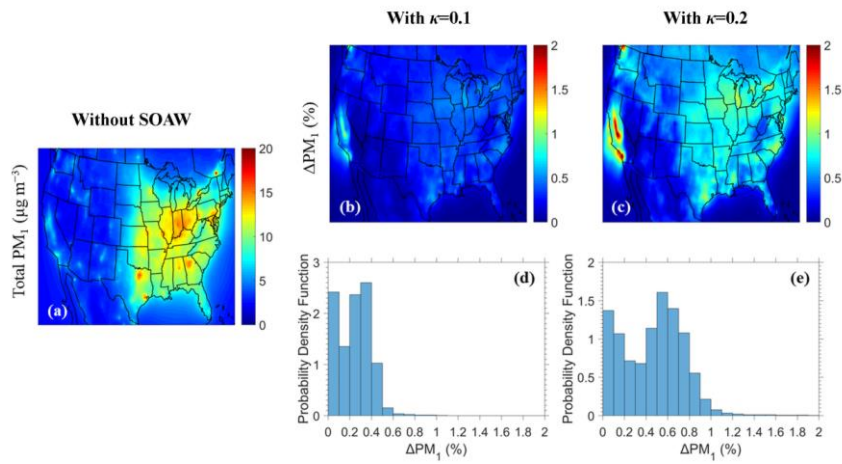
Commented [S26]: Reviewer 1 Comment 19

Commented [S27]: Reviewer 1 Comment 17

542
543
544
545
546
547
548
549
550
551
552
553
554
555

Figure 3. Average ground-level concentrations of PM_{10} water neglecting SOAW (in $\mu\text{g m}^{-3}$) and the fractional increase when SOAW is present in the simulations with $\kappa=0.1$ and $\kappa=0.2$ during: (a) autumn (SON), (b) winter (DJF), (c) spring (MAM), and (d) summer (JJA) of 2010.

556
557

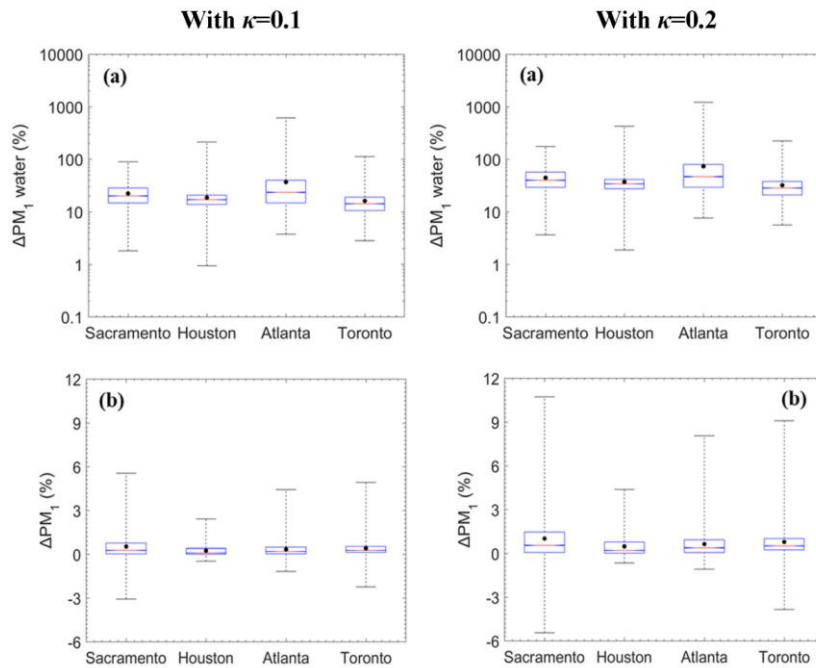


558
559

560 **Figure 42.** Maps of: (a) annual average total dry PM₁ ground-level concentrations
561 neglecting SOAW, (b) annual average fractional increase of total dry PM₁ when
562 SOAW is present in the simulations with $\kappa=0.1$ and, (c) with $\kappa=0.2$ during 2010. The
563 probability density as a function of fractional increase in the annual total dry PM₁
564 concentrations due to SOAW when: (d) $\kappa=0.1$ and (e) $\kappa=0.2$ is shown.

565
566
567
568
569
570
571
572
573
574
575
576
577
578
579
580
581
582
583
584
585
586
587
588

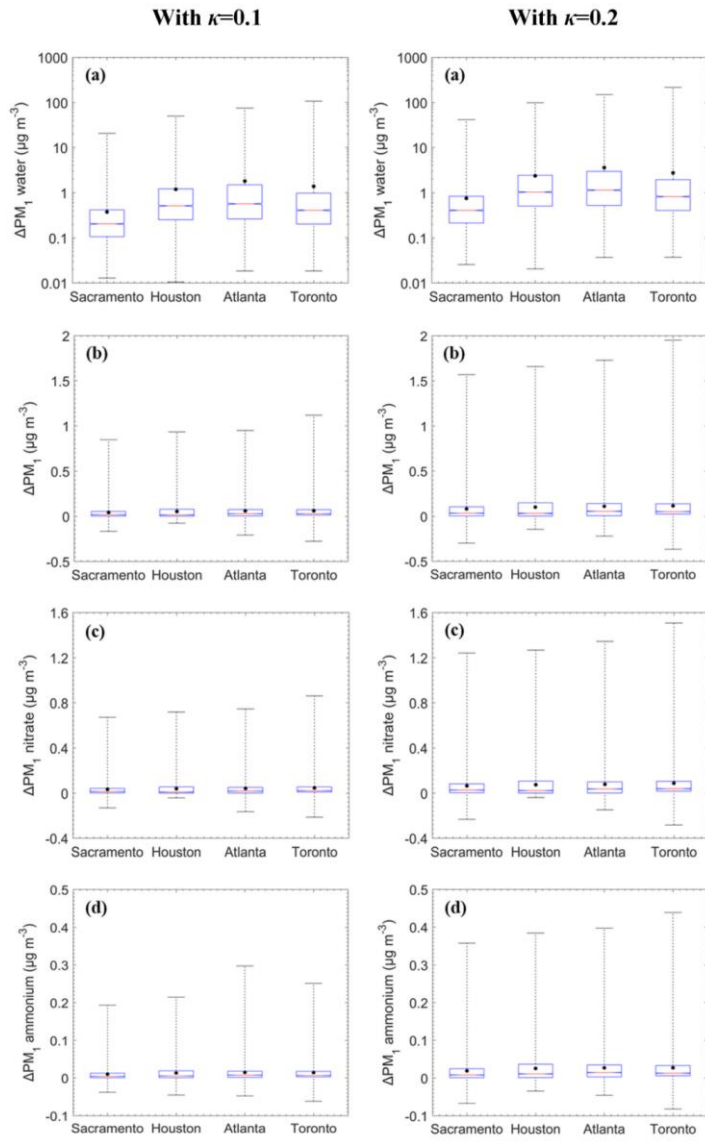
589
590



591
592

593 **Figure 53.** Box plots for fractional change in the hourly: (a) PM₁ water and (b) total
594 dry PM₁ due to SOAW when $\kappa=0.1$ and $\kappa=0.2$ for Sacramento, California; Houston,
595 Texas; Atlanta, Georgia; and Toronto, Canada during 2010. The red line represents
596 the median, the black dot is the mean value, the upper box line is the upper quartile
597 (75%) and the lower box line is the lower quartile (25%) of the distribution. A
598 negative change corresponds to a decrease.

599
600
601
602
603
604
605
606
607
608
609
610
611
612
613

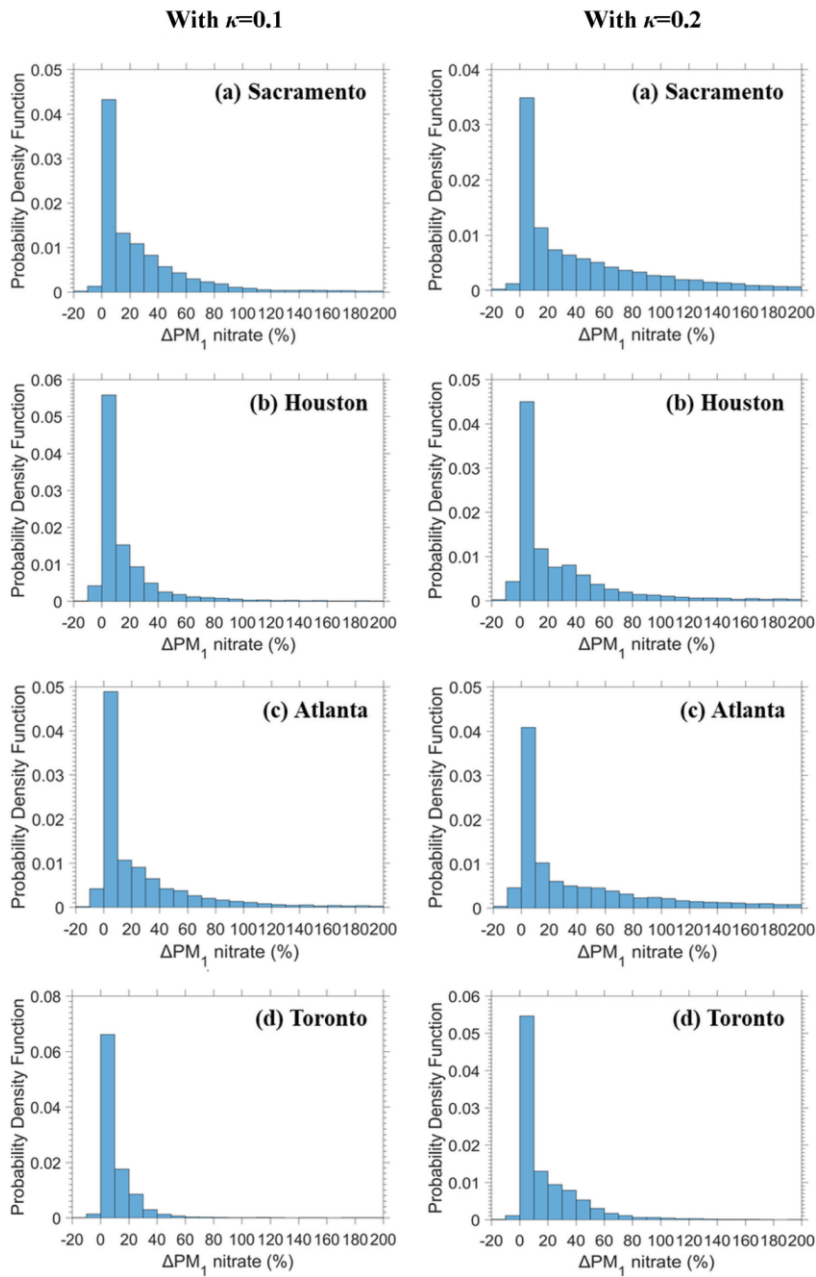


614

615

616 **Figure 6.** Box plots for concentration changes in the hourly PM₁: (a) water, (b) total
 617 dry, (c) nitrate, and (d) ammonium due to SOAW when $\kappa=0.1$ and $\kappa=0.2$ for
 618 Sacramento, California; Houston, Texas; Atlanta, Georgia; and Toronto, Canada
 619 during 2010. The red line represents the median, the black dot is the mean value, the
 620 upper box line is the upper quartile (75%) and the lower box line is the lower quartile
 621 (25%) of the distribution. Water is in log scale to show clearly both the relatively small average and the large range of high
 622 values.

624
625
626
627
628
629
630
631



632
633

634 **Figure 74.** The probability density as a function of fractional increase in the hourly
635 PM_1 nitrate due to SOAW when $\kappa=0.1$ and $\kappa=0.2$ for: (a) Sacramento, California; (b)
636 Houston, Texas; (c) Atlanta, Georgia; and (d) Toronto, Canada during 2010.